

## INDUCING OSCILLATIONS IN A GAS-LIFT BIOREACTOR VIA ANAEROBIC/AEROBIC SWITCHING

**L. F. Calderón-Soto**

Camino a la Presa San José 2055,  
Matemáticas Aplicadas, IPICYT  
S.L.P., México  
luis.calderon@ipicyt.edu.mx

**R. Femat\***

Camino a la Presa San José 2055,  
Matemáticas Aplicadas, IPICYT  
S.L.P., México  
rfemat@ipicyt.edu.mx  
\*Corresponding author

**G. Lara-Cisneros**

Camino a la Presa San José 2055,  
Matemáticas Aplicadas, IPICYT  
S.L.P., México  
gerardo.lara@ipicyt.edu.mx

### Abstract

Bio-photolysis yields diatomic molecules from the breaking of water molecules; this takes place in the thylakoid membrane of some species of algae or cyanobacteria under anaerobic conditions. In anaerobic conditions, there is a consumption of the microorganism intracellular starch pools; thus aerobic conditions are induced to recover the intracellular starch pools and to sustain the bio-photolysis. Under aerobic conditions these microorganisms produce carbohydrates, through CO<sub>2</sub> fixation via *the Calvin cycle*, that are accumulated as starch. In order to carry out both anaerobic/aerobic steps into a process, a gas-lift continuous photobioreactor is supposed such that a mechanism is used to switch between them. As a consequence of the switching, the alternation consumption/accumulation of the intracellular starch pools lead us to investigate oscillatory behavior for a constant dilution rate. Thus, the aim of this work is to determine conditions on switching, with a constant dilution rate, such that the oscillatory behavior occurs into a photobioreactor gas-lift continuous. The equilibria stability analysis was conducted and then the switching effect is studied. Hence, a simple switching rules are proposed to induce oscillatory behavior.

**Keywords:** gas-lift continuous photobioreactor, oscillatory behavior, bio-photolysis, switching.

### 1 Introduction

Current interest in hydrogen technologies entails the need of finding alternative production methods to the natural gas reforming, which requires substantial energy consumption by means of temperatures, pressures and purification of the H<sub>2</sub> [Barba et al., 2008, Hajjaji et al., 2012]. One method with moderated consumption of energy is the biophotolysis, because it occurs under environmental temperature and pressure conditions. The biophotolysis process takes place around the thylakoid membrane of some algae or cyanobacteria [Daday et al., 1977, Berberog et al., 2008], and is developed under anaerobic conditions implying the con-

sumption of the intracellular starch pools, and the reduction of the biomass concentration (see Figure 1.a). Consequently, a regeneration of the biomass is needed to achieve self-sustained operation in biogas production [Hankamer et al., 2007]. Biomass regeneration occurs in aerobic conditions and consists of the CO<sub>2</sub> fixation, dissolved in the medium, via the Calvin cycle and in the subsequent starch accumulation into the intracellular pools [Atomi, 2002] ( see figure 1.b). Both bio-photolysis [Dasgupta et al., 2010] and CO<sub>2</sub> fixation [Kumar and Das, 2012] can be conducted in a gas-lift photobioreactor, and a switching between anaerobic/aerobic conditions suggests the possible oscillatory behavior into the photobioreactor. More details of the bioreactor configuration could be consulted in [Calderón-Soto, 2010].

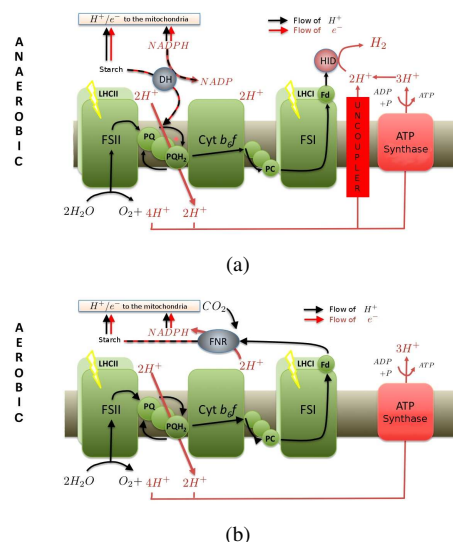


Figure 1. Transmembrane photo-systems in algae or cyanobacteria where occurring: a) Biophotolysis (above); or b) CO<sub>2</sub> fixation (below).

The two processes are light-dependent, due to the inci-

dent photons excite photo-systems I and II (denoted as FSI and FSII in Figure 1) [Melis, 2002]. FSII induces the breaking of the water molecules into the membrane, releasing  $O_2$  and  $H^+$ . In addition, both photo-systems perform a series of redox reactions of the plastocyanin protein and the plastoquinone, (each denoted as PC and PQ, respectively, in Figure 1). Redox reactions generate an electron flow outside of the membrane through FSI and ATP synthase. In bio-photolysis, there is also an electron flow from starch degradation via deshydrogenase (DH in Figure 1.a). The protons generated by the breaking of the water molecules, together with the protons transferred to the membrane by plastoquinone oxidation, are transported out of the membrane by the ATP synthase; this flow is also carried out by the uncoupler action in bio-photolysis (right side of schema at Figure 1). Furthermore, in biophotolysis the flow of electrons and protons is used for  $H_2$  production by the hydrogenase enzyme meanwhile, in  $CO_2$  fixation, such flow is used to produce starch [Hankamer et al., 2007].

The purpose of this study is to determine conditions on the anaerobic/aerobic switching, for a dilution rate value within an appropriated interval, such that the oscillatory behavior is sustained by a gas-lift photobioreactor. To this end, as first step, we analyze separately the existence of solutions for the vector fields under anaerobic and aerobic conditions. For anaerobic condition, the dilution rate value is restricted to satisfy the existence of an unique stable equilibrium point at zero biomass (washout operation). Complementarily, for aerobic condition, the dilution rate value is constrained for a preset biomass concentration value that satisfies the existence of an unique stable operational equilibrium point. Once we have the dilution rate constant belonging to an appropriated interval, the switching is used to induce oscillations towards sustained bio-gas production. The results show that the oscillatory behavior is generated when the  $CO_2$  fixation model is accumulative and the bio-photolysis model is dissipative.

## 2 Analysis of Biophotolysis and $CO_2$ fixation models

We derive the model supposing that temperature, pH, and light intensity are constants along the reactor. The mixing into the reactor is assumed complete for aeration flow [Calderón-Soto, 2010]. Next, dynamics of both biophotolysis and  $CO_2$  fixation are analyzed separately towards the proposal of switching rules.

### 2.1 Biophotolysis model

During bio-photolysis, the starch consumption and water molecules breaking generate a flow of electrons and protons through FSI and FSII (see Figure 1.a). That is, electrons and protons flow is used by the enzyme hydrogenase to produce  $H_2$  under anaerobic stress. Henceforth, we can consider that the starch concentration in the liquid phase is the substrate and the  $H_2$  concentration is the product. It should be noted that the

bio-photolysis exhibits inhibition phenomena by substrate [Lee et al., 2007] as well as product [Melis and Happe, 2001]. In addition, since the  $H_2$  is not a primary metabolite and has not primary precursors its yielding is non-growth associated. Under these facts and from the mass balance for  $H_2$  concentration in liquid phase ( $x_1$ ), biomass concentration in liquid phase ( $x_2$ ) and starch concentration in liquid phase ( $x_3$ ); an unstructured model is formulated. Although validity and limitations of a specific kinetic growth rate and parameters values deserve discussion, we actually model the bio-photolysis dynamics in a general framework, which is argued from the above facts with only general properties on kinetic growth rate.

The dynamical system for bio-photolysis dynamics is proposed as  $\dot{z}_1 = f_1(z_1)$  with  $z_1(t_{0_1}) = z_{1_0}$ , where  $z_1 = [x_1, x_2, x_3]^T \in \mathbb{R}_{\geq 0}^3$  and:

$$f_1(z_1) = \begin{pmatrix} \beta x_2 - D x_1 \\ (\mu_1(x_3, x_1) - D)x_2 \\ -\frac{\mu_1(x_3, x_1)}{Y_1} x_2 - D x_3 \end{pmatrix} \quad (1)$$

where  $D$  is the ratio between supply flow with reactor volume that is named dilution rate,  $Y_1$  and  $\beta$  are real positive scalars which denote the biomass/ $CO_2$  yield coefficient and the non-growth associated product generation coefficient, respectively, and the function  $\mu_1$  stands for the specific growth rate of the bio-photolysis process. Being its parameter space:  $\kappa_1 = \{(D, Y_1, \beta, K_{s_1}, K_{p_1}) | D \in \mathbb{R}_+, Y_1 \in \mathbb{R}_+, \beta \in \mathbb{R}_+, K_{s_1} \in \mathbb{R}_+^o, K_{p_1} \in \mathbb{R}_+^r\}$ . The state components belong to value sets:  $\mathfrak{X}_1 = \{x_1 \in \mathbb{R} | 0 \leq x_1 \leq H_m\}$ ,  $\mathfrak{X}_2 = \{x_2 \in \mathbb{R} | 0 \leq x_2 \leq X_m\}$  and  $\mathfrak{X}_3 = \{x_3 \in \mathbb{R} | 0 \leq x_3 \leq C_m\}$ ; where  $H_m$  stands for the  $H_2$  thermodynamical equilibrium concentration at liquid phase, and  $X_m$  and  $C_m$  stands for the maximum biomass and starch reachable concentrations, respectively. Thus, the system domain becomes  $\Omega_1 = \{(x_1, x_2, x_3) \in \mathbb{R}^3 | x_1 \in \mathfrak{X}_1, x_2 \in \mathfrak{X}_2, x_3 \in \mathfrak{X}_3\}$ .

### 2.2 $CO_2$ fixation model

The  $CO_2$  fixation is a step of the Calvin-cycle carried out by the RUBISCO enzyme, and consists on the incorporation of the  $CO_2$  to one pentose and the lysis of this last one into two trioses, whose after some steps of the cycle are phosphorylated and then bonded to yield phosphorylated glucose that is polymerized and stored as starch into the intracellular pools [Atomi, 2002]. Based on this, we assume that the concentration of  $CO_2$  dissolved is the substrate whereas the concentration of starch dissolved is the product. The  $CO_2$  fixation could be modeled as a bioprocess with a specific growth rate with substrate inhibition [Kurano and Miyachi, 2005]. Product inhibition is associated to starch accumulation,

which affects the photosynthetic activity. Product inhibition is attributable also to the physical disrupt of the CO<sub>2</sub> diffusion through the chloroplasts caused by the great amount of the polymer that can occur by its slow consumption [Sawada et al., 2001, Stitt, 1991]. Additionally, carbohydrates are primary metabolites therefore the product generation is associated to the growth. The CO<sub>2</sub> equilibrium concentration in liquid phase of the inlet gas diffused by bubbling is calculated with the Henry law, assuming that the inlet gas saturates the medium. The Henry law relates linearly the partial pressure ( $p$ ) in gas phase of the compound that is being diluted in the medium, with its molar concentration in liquid phase, by the Henry constant ( $k_H$ ) [Masterton and Hurley, 2008]. System pressure is the environment standard and then partial pressure of CO<sub>2</sub> is the molar fraction in gas phase. Thus the thermodynamical equilibrium for the concentration of CO<sub>2</sub> in liquid phase is

$$x_{4f} = x_{4in} W_{CO_2} k_H = \sigma x_{4in} \quad (2)$$

where  $W_{CO_2}$  is the CO<sub>2</sub> molar weight,  $x_{4in}$  is the gas inlet partial pressure and ( $x_{4f}$ ) stands for the CO<sub>2</sub> equilibrium concentration in liquid phase (see details in modeling at [Trambouze and Euzen, 2004]).

The process model is derived from the mass balance for CO<sub>2</sub> concentration in liquid phase ( $x_4$ ), biomass concentration in liquid phase ( $x_2$ ), and starch concentration in liquid phase ( $x_3$ ). Henceforth, mass balance renders in a system  $\dot{z}_2 = f_2(z_2)$  with  $z_2(t_{0_2}) = z_{2_0}$ , where  $z_2 = (x_4, x_2, x_3)^T$ , with

$$f_2(z_2) = \begin{pmatrix} k_{La}(x_{4f} - x_4) - \frac{\mu_2(x_4, x_3)}{Y_2} x_2 - D x_4 \\ (\mu_2(x_4, x_3) - D) x_2 \\ \alpha \mu_2(x_4, x_3) x_2 - D x_3 \end{pmatrix} \quad (3)$$

where  $Y_2$  is the biomass/starch yield coefficient,  $\alpha$  is the growth associated product generation coefficient, and  $k_{La}$  the CO<sub>2</sub> mass transfer coefficient, being all of them positive constants, and the function  $\mu_2$  represents specific growth rate of the CO<sub>2</sub> fixation bioprocess. Being its parameter space  $\kappa_2 = \{(D, k_{La}, x_{4f}, Y_2, \alpha, K_{s_2}, K_{p_2}) | D \in \mathbb{R}_+, x_{4f} \in \mathbb{R}_+, Y_2 \in \mathbb{R}_+, \alpha \in \mathbb{R}_+, K_{s_2} \in \mathbb{R}_+^p, K_{p_2} \in \mathbb{R}_+^q\}$ . The value sets of state variables are:  $\hat{\mathcal{X}}_4 = \{x_4 \in \mathbb{R} | 0 \leq x_4 \leq x_{4f}\}$ ,  $\hat{\mathcal{X}}_2$  and  $\hat{\mathcal{X}}_3$ . Thus, the system domain becomes  $\Omega_2 = \{(x_4, x_2, x_3) \in \mathbb{R}^3 | x_4 \in \hat{\mathcal{X}}_4, x_2 \in \hat{\mathcal{X}}_2, x_3 \in \hat{\mathcal{X}}_3\}$ .

### 2.3 Analysis

Let us define  $\hat{z}_1 := (\hat{x}_1, \hat{x}_2, \hat{x}_3)^T = (x_1/H_m, x_2/Y_2 x_{4f}, x_3/\alpha Y_2 x_{4f})^T$  to derive the dimensionless expression for (1) as follows:

$$\hat{f}_1(\hat{z}_1) = \begin{pmatrix} \hat{\beta} \hat{x}_2 - \hat{D} \hat{x}_1 \\ (\hat{\mu}_{s_1}(\hat{x}_3) \hat{\mu}_{p_1}(\hat{x}_1) - \hat{D}) \hat{x}_2 \\ \delta \hat{\mu}_{s_1}(\hat{x}_3) \hat{\mu}_{p_1}(\hat{x}_1) \hat{x}_2 - \hat{D} \hat{x}_3 \end{pmatrix} \quad (4)$$

where  $\hat{\mu}_{s_1} = \frac{\mu_{s_1}}{\mu_{s_2}}$ ,  $\hat{\beta} = \frac{\beta Y_1 C_m}{H_m \mu_{s_2}}$ ,  $\delta = \frac{1}{\alpha Y_1}$  and  $\hat{D} = \frac{D}{\mu_{s_2}}$ . The domain is  $\hat{\Omega}_1 = \{(\hat{x}_1, \hat{x}_2, \hat{x}_3) \in \mathbb{R}^3 | \hat{x}_1 \in \hat{\mathcal{X}}_1, \hat{x}_2 \in \hat{\mathcal{X}}_2, \hat{x}_3 \in \hat{\mathcal{X}}_3\}$ , with  $\hat{\mathcal{X}}_1 = \{\hat{x}_1 \in \mathbb{R} | 0 \leq \hat{x}_1 \leq 1\}$ ,  $\hat{\mathcal{X}}_2 = \{\hat{x}_2 \in \mathbb{R} | 0 \leq \hat{x}_2 \leq \hat{X}_m\}$  and  $\hat{\mathcal{X}}_3 = \{\hat{x}_3 \in \mathbb{R} | 0 \leq \hat{x}_3 \leq \hat{C}_m\}$ , where  $\hat{X}_m = \frac{X_m}{Y_2 x_{4f}}$  and  $\hat{C}_m = \frac{C_m}{\alpha Y_2 x_{4f}}$ ; being the dimensionless parameter vector  $\hat{\kappa}_1 = \{(\hat{D}, \hat{\beta}, \hat{K}_{s_1}, \hat{K}_{p_1}) | \hat{D} \in \mathbb{R}_+, \hat{\beta} \in \mathbb{R}_+, \delta \in \mathbb{R}_+, \hat{K}_{s_1} \in \mathbb{R}_+^p, \hat{K}_{p_1} \in \mathbb{R}_+^q\}$ .

Defining  $\hat{z}_2 := (\bar{x}_4, \bar{x}_2, \bar{x}_3)^T = (x_4/x_{4f}, x_2/Y_2 x_{4f}, x_3/\alpha Y_2 x_{4f})^T$ , obtaining the dimensionless system of (3) as:

$$\hat{f}_2(\hat{z}_2) = \begin{pmatrix} \hat{k}_{La}(1 - \hat{x}_4) - \hat{\mu}_{s_2}(\hat{x}_4) \hat{\mu}_{p_2}(\hat{x}_3) \hat{x}_2 - \hat{D} \hat{x}_4 \\ (\hat{\mu}_{s_2}(\hat{x}_4) \hat{\mu}_{p_2}(\hat{x}_3) - \hat{D}) \hat{x}_2 \\ \hat{\mu}_{s_2}(\hat{x}_4) \hat{\mu}_{p_2}(\hat{x}_3) \hat{x}_2 - \hat{D} \hat{x}_3 \end{pmatrix} \quad (5)$$

where  $\hat{\mu}_{s_2} = \frac{\mu_{s_2}}{\mu_{s_2}}$  and  $\hat{k}_{La} = \frac{k_{La}}{\mu_{s_2}}$ . The domain for the dimensionless model is re-written as  $\hat{\Omega}_2 = \{(\hat{x}_4, \hat{x}_2, \hat{x}_3) \in \mathbb{R}^3 | \hat{x}_4 \in \hat{\mathcal{X}}_4, \hat{x}_2 \in \hat{\mathcal{X}}_2, \hat{x}_3 \in \hat{\mathcal{X}}_3\}$ , with:  $\hat{\mathcal{X}}_4 = \{\hat{x}_4 \in \mathbb{R} | 0 \leq \hat{x}_4 \leq 1\}$ ; being the dimensionless parameter vector  $\hat{\kappa}_2 = \{(\hat{D}, \hat{k}_{La}, \hat{K}_{s_2}, \hat{K}_{p_2}) | \hat{D} \in \mathbb{R}_+, \hat{k}_{La} \in \mathbb{R}_+, \hat{K}_{s_2} \in \mathbb{R}_+^p, \hat{K}_{p_2} \in \mathbb{R}_+^q\}$ .

We assume that  $\hat{\mu}_1$  and  $\hat{\mu}_2$  include, each one, the substrate and product inhibition phenomena via variable separation functions, *i.e.*,  $\hat{\mu}_1(\hat{x}_3, \hat{x}_1) = \hat{\mu}_{s_1}(\hat{x}_3) \hat{\mu}_{p_1}(\hat{x}_1)$  and  $\hat{\mu}_2(\hat{x}_4, \hat{x}_3) = \hat{\mu}_{s_2}(\hat{x}_4) \hat{\mu}_{p_2}(\hat{x}_3)$ . Moreover, we suppose functions  $\hat{\mu}_{s_i}$  and  $\hat{\mu}_{p_i}$  have the following properties:

1.  $\hat{\mu}_{s_i} \in C^l(\hat{\mathcal{X}}_j)$ ,  $\hat{\mu}_{p_i} \in C^l(\hat{\mathcal{X}}_k)$ , for at least  $l = 1$ .
2.  $\hat{\mu}_{s_i}(0) = 0$  and  $\forall \hat{x}_j \in \hat{\mathcal{X}}_j$ ,  $0 \leq \hat{\mu}_{s_i}(\hat{x}_j) \leq \hat{\mu}_{s_i}$ . In addition,  $\exists \hat{x}_j^* \in \hat{\mathcal{X}}_j \ni \hat{\mu}'_{s_i}(\hat{x}_j^*) = 0$  and  $\forall \hat{x}_j \in [0, \hat{x}_j^*]$ ,  $\hat{\mu}'_{s_i} > 0$ , while  $\forall \hat{x}_j \in (\hat{x}_j^*, \max\{\hat{\mathcal{X}}_j\}]$ ,  $\hat{\mu}'_{s_i} < 0$ , where  $\hat{\mu}'_{s_i}(\hat{x}_j) = \frac{d\hat{\mu}_{s_i}(\hat{x}_j)}{d\hat{x}_j}$  and  $|\hat{\mu}'_{s_i}| < \tilde{\mu}'_{s_i}$ .
3.  $\hat{\mu}_{p_i}(0) = 1$  and  $0 \leq \hat{\mu}_{p_i}(\hat{x}_k) \leq 1$ ,  $\forall \hat{x}_k \in \hat{\mathcal{X}}_k$ . Furthermore,  $\forall \hat{x}_k \in \hat{\mathcal{X}}_k$ ,  $\hat{\mu}'_{p_i} < 0$  where  $\hat{\mu}'_{p_i}(\hat{x}_k) = \frac{d\hat{\mu}_{p_i}(\hat{x}_k)}{d\hat{x}_k}$  and  $|\hat{\mu}'_{p_i}| < \tilde{\mu}'_{p_i}$ .

For  $j = 3$  and  $k = 1$  when  $i = 1$ , and for  $j = 4$  and  $k = 3$  when  $i = 2$ .

Since  $\hat{\mu}_{s_1}$  and  $\hat{\mu}_{s_2}$  have the Properties 1-3,  $\hat{f}_1$  and  $\hat{f}_2$  are at least  $C^1$  then from the Lemma 3.2 of [Khalil, 2002] the systems (4) and (5) have a unique solution,

each one. Regarding the equilibrium points and their stability we have the statements after the next condition paragraph.

The desirable operation conditions for both processes include a large residence time of the microorganism in the reactor, with this aim the dilution rate value must be low. In the Biophotolysis the product generation period increases with the residence time. The CO<sub>2</sub> fixation is catalyzed by the RUBISCO enzyme that has a turnover rate about  $2 - 5s^{-1}$ , too much slow for an enzyme [Atomi, 2002], then a large residence time improves the process efficiency. Therefore we assume  $\hat{D} < \hat{\mu}_{s_2}(1)$ .

**Proposition 2.1.** *The system (4) has a unique equilibrium point  $\hat{z}_1 = (0, 0, 0)$  and it is locally stable in  $\hat{\Omega}_1$ .*

*Proof.* From  $\hat{f}_1(\hat{x}_{1j}, \hat{x}_{2j}, \hat{x}_{3j}) = (0, 0, 0)$  there are two forms of equilibrium points:  $\hat{z}_{1_1} = (0, 0, 0)$  if  $\hat{x}_2 = 0$ , and  $\hat{z}_{1_j} = \left(-\frac{\hat{\beta}}{\hat{\delta}\hat{D}}\hat{x}_{3_j}, -\frac{\hat{x}_{3_j}}{\hat{\delta}}, \hat{x}_{3_j}\right)$  if  $\hat{D} = \hat{\mu}_{s_1}(\hat{x}_{3_j})\hat{\mu}_{p_1}\left(-\frac{\hat{\beta}}{\hat{\delta}\hat{D}}\hat{x}_{3_j}\right)$ ; but the latter form of equilibrium points implies that one or two of its coordinates are negatives and then no one  $\hat{z}_{1_j}$  is in  $\hat{\Omega}_1$  for  $j > 1$ , in consequence the point  $\hat{z}_{1_1}$  is unique in  $\hat{\Omega}_1$ . Evaluating jacobian matrix of (4) in this point results:

$$\left.\frac{\partial \hat{f}}{\partial \hat{z}_1}\right|_{\hat{z}_{1_1}} = \begin{bmatrix} -\hat{D} & \hat{\beta} & 0 \\ 0 & -\hat{D} & 0 \\ 0 & 0 & -\hat{D} \end{bmatrix};$$

whose eigenvalues are  $\lambda_{1,2,3} = -\hat{D}$ . Since  $\hat{D}$  is positive, therefore  $\hat{z}_{1_1}$  is locally stable.

**Proposition 2.2.** *Assuming that  $\hat{k}_{La} \gg \hat{\mu}_{s_2}(1) > \hat{D}$ , the system (5) has two equilibrium points: the washout equilibrium point  $\hat{z}_{2_1} \approx (1, 0, 0)^T$  that is a saddle node and an operational equilibrium point  $\hat{z}_{2_2} = \left(\hat{x}_{4_2}, \frac{\hat{k}_{La}}{\hat{D}}(1 - \hat{x}_{4_2}) - \hat{x}_{4_2}, \frac{\hat{k}_{La}}{\hat{D}}(1 - \hat{x}_{4_2}) - \hat{x}_{4_2}\right)$  that is locally stable in  $\hat{\Omega}_2$ .*

*Proof.* From  $\hat{f}_2(\hat{x}_{4_j}, \hat{x}_{2_j}, \hat{x}_{3_j}) = (0, 0, 0)$  exists two forms of equilibrium points:  $\hat{z}_{2_1} = \left(\frac{\hat{k}_{La}}{\hat{D} + \hat{k}_{La}}, 0, 0\right) \approx (1, 0, 0)$  if  $\hat{x}_2 = 0$ , and  $\hat{z}_{2_j} = \left(\hat{x}_{4_j}, \frac{\hat{k}_{La}}{\hat{D}}(1 - \hat{x}_{4_j}) - \hat{x}_{4_j}, \frac{\hat{k}_{La}}{\hat{D}}(1 - \hat{x}_{4_j}) - \hat{x}_{4_j}\right)$  if  $\hat{D} = \hat{\mu}_{s_2}(\hat{x}_{4_j})\hat{\mu}_{p_2}\left(\frac{\hat{k}_{La}}{\hat{D}}(1 - \hat{x}_{4_j}) - \hat{x}_{4_j}\right)$ .

From the assumption  $\hat{\mu}_{s_2}(1) > \hat{D}$ , the equation  $\hat{D} = \hat{\mu}_{s_2}(\hat{x}_{4_j})\hat{\mu}_{p_2}\left(\frac{\hat{k}_{La}}{\hat{D}}(1 - \hat{x}_{4_j}) - \hat{x}_{4_j}\right)$  has only one solution  $\hat{x}_{4_2}$ , since the product  $\hat{\mu}_{s_2}\hat{\mu}_{p_2}$  has one or no maximum ( $\hat{x}_4^{**}$ ) in  $\hat{\Omega}_2$ , this is because  $\hat{\mu}_{p_2}$  reduces the value of  $\hat{\mu}_{s_2}$ , and as both are smooth, the maximum of the product is moved rightward and could be out of the domain. Based on the same assumption  $\hat{x}_{4_2}$  has a value under  $\hat{x}_4^{**}$ , and then by the chain rule and the maximum properties:

$$\begin{aligned} \frac{d\left(\hat{\mu}_{s_2}(\hat{x}_{4_2})\hat{\mu}_{p_2}\left(\frac{\hat{k}_{La}}{\hat{D}}(1 - \hat{x}_{4_2}) - \hat{x}_{4_2}\right)\right)}{d\hat{x}_{4_2}} &= \\ \hat{\mu}'_{s_2}(\hat{x}_{4_2})\hat{\mu}_{p_2}\left(\frac{\hat{k}_{La}}{\hat{D}}(1 - \hat{x}_{4_2}) - \hat{x}_{4_2}\right) &- \\ \hat{\mu}'_{p_2}\left(\frac{\hat{k}_{La}}{\hat{D}}(1 - \hat{x}_{4_2}) - \hat{x}_{4_2}\right)\hat{\mu}_{s_2}(\hat{x}_{4_2})\left(1 + \frac{\hat{k}_{La}}{\hat{D}}\right) &= \\ a - b\left(1 + \frac{\hat{k}_{La}}{\hat{D}}\right) &> 0 \end{aligned}$$

Applying the Lyapunov indirect method:

$$\begin{aligned} \left.\frac{\partial \hat{f}_2}{\partial \hat{z}_2}\right|_{\hat{z}_{2_1}} &= \begin{bmatrix} -(\hat{D} + \hat{k}_{La}) & -\hat{\mu}_{s_2}(1) & 0 \\ 0 & \hat{\mu}_{s_2}(1) - \hat{D} & 0 \\ 0 & \hat{\mu}_{s_2}(1) & -\hat{D} \end{bmatrix} \\ \text{eigenvalues : } &\left\{ \begin{array}{l} \lambda_{1_1} = -(\hat{D} + \hat{k}_{La}) \\ \lambda_{2_1} = \hat{\mu}_{s_2}(1) - \hat{D} \\ \lambda_{3_1} = -\hat{D} \end{array} \right\} \\ \left.\frac{\partial \hat{f}_2}{\partial \hat{z}_2}\right|_{\hat{z}_{2_j}} &= \begin{bmatrix} -bc - d - \hat{D} & -bc \\ ac & 0 & bc \\ ac & \hat{D} & bc - \hat{D} \end{bmatrix} \\ \text{where : } &\left\{ \begin{array}{l} a = \hat{\mu}'_{s_2}(\hat{x}_{4_2})\hat{\mu}_{p_2}(c) \\ b = \hat{\mu}'_{p_2}(c)\hat{\mu}_{s_2}(\hat{x}_{4_2}) \\ c = \frac{\hat{k}_{La}}{\hat{D}}(1 - \hat{x}_{4_2}) - \hat{x}_{4_2} \\ d = -bc + ac + \hat{k}_{La} + \hat{D} \end{array} \right\} \\ \text{eigenvalues : } &\left\{ \begin{array}{l} \lambda_{1_2} = -\hat{D} \\ -d \left( 1 \pm \sqrt{1 - \frac{4c\hat{D}(a-b(1+\frac{\hat{k}_{La}}{\hat{D}}))}{d^2}} \right) \\ \lambda_{2,3_2} = \frac{\quad}{2} \end{array} \right\} \end{aligned}$$

Therefore, as  $0 < \hat{D} \leq \hat{\mu}_{s_1}(1)$  is haven that  $\lambda_{2_1} > 0 > \lambda_{3_1} > \lambda_{1_1}$  and then  $\hat{z}_{1_1}$  is a saddle point, and as  $0 < 4c\hat{D}\frac{a-b(1+\frac{\hat{k}_{La}}{\hat{D}})}{d^2}$  is haven that  $\lambda_{1_2} < 0$  and the real parts of  $\lambda_{2_2}$  and  $\lambda_{3_2}$  are negatives, then  $\hat{z}_{2_2}$  is locally stable in  $\hat{\Omega}_2$

**Remark 2.3.** *If  $\hat{D} > \hat{\mu}_{s_2}$  the washout equilibrium of (5) would be unique and stable, since  $\hat{D} = \hat{\mu}_{s_2}(\hat{x}_{4_j})\hat{\mu}_{p_2}\left(\frac{\hat{k}_{La}}{\hat{D}}(1 - \hat{x}_{4_j}) - \hat{x}_{4_j}\right)$  would have no solution in  $\hat{\Omega}_2$  and  $0 > \lambda_{2_2} > \lambda_{3_2} > \lambda_{1_2}$*

### 3 Switching induces oscillatory behavior

In both processes, the biomass concentration is the easiest to measure. From the process dynamics description, is deduced that high concentration of biomass is needed to begin the biophotolysis process, and when the biomass is low its recovery becomes necessary. Based on these facts, the biomass concentration is the state variable used as a switching criterion, with two values: ( $x_{2_{\max}}$ ) that is sufficient to begin the biophotolysis and ( $x_{2_{\min}}$ ) at which is necessary the beginning of the biomass regeneration. As  $x_{2_{\min}}$  is lower the starch pool consumption and the biomass reduction are greater and could cause that regeneration will be not longer able. The value  $x_{2_{\max}}$  only must be less than

$\bar{x}_{2_2}$ , the second coordinate of the operational equilibrium point of (3).

The switching mechanism (6) was formulated under the desirable operation conditions, that is, when biomass concentration value is less than  $x_{2_{\min}}$ , the mechanism switches from anaerobic to aerobic conditions to begin biomass regeneration; when it is greater than  $x_{2_{\max}}$ , the mechanism switches from aerobic to anaerobic conditions and bio-photolysis takes place. When biomass concentration is between  $x_{2_{\min}}$  and  $x_{2_{\max}}$ , is supposed that the second equation of (3) is positive and the second of (1) is negative, that is, between these values  $f_2$  is accumulative for  $x_2$  and  $f_1$  is dissipative for  $x_2$ .

$$F(Z) = \left\{ \begin{array}{ll} f_1 \text{ if} & x_2 \leq x_{2_{\min}} \\ & \vee \left( x_{2_{\min}} < x_2 < x_{2_{\max}} \wedge \frac{dF_2}{dx_2} > 0 \right) \\ f_2 \text{ if} & x_2 \geq x_{2_{\max}} \\ & \vee \left( x_{2_{\min}} < x_2 < x_{2_{\max}} \wedge \frac{dF_2}{dx_2} < 0 \right) \end{array} \right\} \quad (6)$$

The switching mechanism constraints the  $f_1$  and  $f_2$  domains on their  $x_2$  coordinate, in consequence the unique equilibrium point of  $f_1$  lays out of its constrained domain which points inside of itself on all of its frontiers except on the plane  $\Gamma_1 = \{(x_1, x_2, x_3) | x_1 \in \mathfrak{X}_1, x_2 = x_{2_{\min}}, x_3 \in \mathfrak{X}_3\}$ , on the other hand the operational equilibrium point of  $f_2$  lays out of its constrained domain which points inside of itself on all of its frontiers except on the plane  $\Gamma_2 = \{(x_4, x_2, x_3) | x_4 \in \mathfrak{X}_4, x_2 = x_{2_{\max}}, x_3 \in \mathfrak{X}_3\}$ . Therefore, the switching between  $f_1$  and  $f_2$  induces that the trajectories do not arise the stable equilibrium points of each vector field, thus the trajectories are kept in the region between  $\Gamma_1$  and  $\Gamma_2$  (see figure 2). This leads us to consider that the system has an oscillatory behavior.

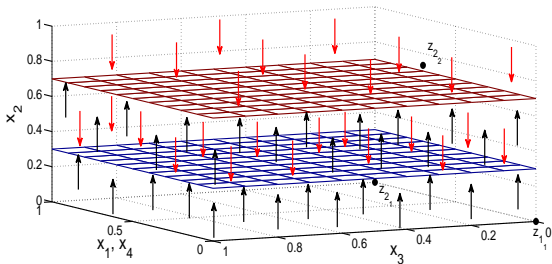
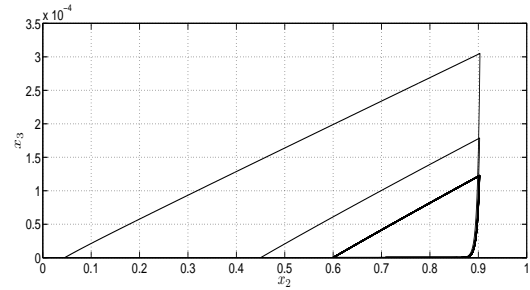


Figure 2. The trajectories of the switched system are contained by the switching planes  $\Gamma_1$  and  $\Gamma_2$  for no initial condition between them. The red and black arrows represent the  $\hat{f}_1$  and  $\hat{f}_2$  field vector directions, respectively, and the planes blue and red represent  $\Gamma_1$  and  $\Gamma_2$ , respectively.

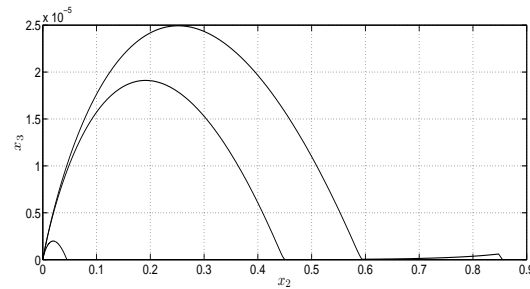
## 4 Numerical Simulations

The oscillatory behavior and the washout are illustrated in this section with graphics of the numeric simulation. The functions that represent the inhibition phenomena and conform the specific growth rate for this simulations are for the both models:  $\mu_{s_i}(S) = \frac{\mu_{max_i} S}{k_{S_i} + S + \frac{S^2}{k_{I_i}}}$  and  $\mu_{p_i}(P) = \left(1 - \frac{P}{k_{P_i}}\right)^{\gamma_i}$ . Being the parameters:  $K_{s_i} = \{k_{S_i}, k_{I_i}, \mu_{max_i}\}$  and  $K_{p_i} = \{k_{P_i}, \gamma_i\}$ , both for  $i = 1$  and  $i = 2$ . In [Reger et al., 2009] the Henry constant value for  $\text{CO}_2$ , in water, reported is  $k_H = 31.3 \frac{mM}{atm}$ , and in [Moore et al., 2009] is  $k_H = 44 \frac{\mu M}{mmHg} * 760 \frac{mmHg}{atm} = 33.44 \frac{mM}{atm}$ , in this section we use the arithmetic mean of both values  $32.37 \frac{mM}{atm}$ , then  $\sigma = 44 \frac{\mu M}{mol} * 0.03237 \frac{mol}{L atm}$ . The  $\text{CO}_2$  inlet partial pressure is  $x_{4in} = 0.04$  thus  $x_{4f} = \sigma x_{4in} = 0.0568 \frac{g_{x_4}}{L atm}$ . This value was used only as approximation, because the medium employed for both process has salt compounds in dissolution [Tsygankov et al., 2002], then the values of  $k_H$  varies.

The parameter vectors for the simulations are:  $\kappa_{1_i} = (D_i, 19.25hr^{-1}, 0.194 \frac{g_{x_2}}{g_{x_3}}, 0.000155hr^{-1}, 0.66 \frac{g_{x_3}}{L}, 50.315 \frac{g_{x_3}}{L}, 0.123hr^{-1}, 1.880 \frac{g_{x_4}}{L}, 3.656)$  and  $\kappa_{2_i} = (D_i, 0.0568 \frac{g_{x_4}}{L atm}, 0.5 \frac{g_{x_2}}{g_{x_4}}, 0.347 \frac{mg_{x_3}}{g_{x_2}}, 0.334 \frac{g_{x_4}}{L}, 30 \frac{g_{x_4}}{L}, 0.385hr^{-1}, 8.314 \frac{mg_{x_3}}{L}, 3.101)$ . The figure 3.a) shows the oscillatory behavior for  $D_1 = 0.005hr^{-1}$ , while the figure 3.b) shows the washout with  $D_2 = 0.105hr^{-1}$ .



(a)



(b)

Figure 3. Projection of the phase space over  $x_2 - x_3$  of the complete process: a) For  $D < \mu_{s_1}(x_{4f})$  the system exhibits oscillatory behavior, b) For  $D > \mu_{max_2}$  the reactor washes out.

## 5 Conclusions

This paper contributes on the analysis of a bio-inspired oscillator, which arises from a mechanism that switches between two operating conditions into a photobioreactor. The operating conditions correspond to aerobic and anaerobic regimes, the aerobic regime induces CO<sub>2</sub> fixation whereas the anaerobic regime leads to biophotolysis. The parameter values of vector fields in both operating regime models and the switching rule are such that there are two behaviors: oscillatory and washout, for the previously described low and high values of the dilution rate respectively. Numerical simulations of the section 4 illustrate both behaviors.

Based on the analysis developed in section 2 and the mechanism description in the section 3, the suggested operative procedure is:

1. Starting with biomass and CO<sub>2</sub> concentration, in the liquid phase, initial conditions with low values and practically null for the starch.
2. Maintain a constant dilution rate value under  $\mu_{s_2}(1)$ , with the option to reduce this value with the switching from  $f_2$  to  $f_1$ , and re-establish it with the switching from  $f_1$  to  $f_2$ .
3. Finish the process inducing the washout with the increase of the dilution rate value.

## 6 Acknowledgements

L.F. Calderón-Soto thanks CONACYT for the scholarship grant number 215868.

## References

- Atomi, H. (2002). Microbial enzymes involved in carbon dioxide fixation. *Journal of Bioscience and Bioengineering*, 94(6):497–505.
- Barba, D., Giacobbe, F., Cesaris, A. D., Farace, A., Iaquaniello, G., and Pipino, A. (2008). Membrane reforming in converting natural gas to hydrogen (part one). *International Journal of Hydrogen Energy*, 33(14):3700 – 3709.
- Berberog, H., Barra, N., Pilon, L., and Jay, J. (2008). Growth, CO<sub>2</sub> consumption and H<sub>2</sub> production of *Anabaena variabilis* ATCC 29413-U under different irradiances and CO<sub>2</sub> concentrations. *Journal of Applied Microbiology*, 104:105–121.
- Calderón-Soto, L. F. (2010). Diseño, instrumentación y caracterización abiótica de un sistema para la bioproducción de hidrógeno. Master's thesis, Universidad Politécnica de Pachuca.
- Daday, A., Platz, R. A., and Smith, G. D. (1977). Anaerobic and aerobic hydrogen gas formation by the blue-green alga *Anabaena cylindrica*. *Applied and Environmental Microbiology*, 34(5):478–483.
- Dasgupta, C. N., Gilbert, J. J., Lindblad, P., Heidorn, T., Borgvang, S. A., Skjanes, K., and Das, D. (2010). Recent trends on the development of photobiological processes and photobioreactors for the improvement of hydrogen production. *international journal of hydrogen energy*, 35(19):10218–10238.
- Hajjaji, N., Pons, M.-N., Houas, A., and Renaudin, V. (2012). Exergy analysis: An efficient tool for understanding and improving hydrogen production via the steam methane reforming process. *Energy Policy*, 42(0):392 – 399.
- Hankamer, B., Lehr, F., Rupprecht, J., Mussnug, J. H., Posten, C., and Kruse, O. (2007). Photosynthetic biomass and H<sub>2</sub> production by green algae: from bioengineering to bioreactor scale-up. *Physiologia plantarum*, 131(1):10–21.
- Khalil, H. (2002). *Nonlinear systems*. Prentice Hall, Upper Saddle River, N.J., 3rd edition.
- Kumar, K. and Das, D. (2012). Growth characteristics of chlorella sorokiniana in airlift and bubble column photobioreactors. *Bioresource Technology*, 116(0):307 – 313.
- Kurano, N. and Miyachi, S. (2005). Selection of microalgal growth model for describing specific growth rate-lite response using extended information criterion. *Journal of Bioscience and Bioengineering*, 100(4):403–408.
- Lee, J. Z., Klaus, D., Maness, P.-C., and Spea, J. (2007). The effect of butyrate concentration on hydrogen production via photofermentation for use in a martian habitat resource recovery process. *International Journal of Hydrogen Energy*, 32(15):3301 – 3307.
- Masterton, W. and Hurley, C. (2008). *Chemistry: Principles and Reactions*. Available Titles CengageNOW Series. Cengage Learning.
- Melis, A. (2002). Green alga hydrogen production: progress, challenges and prospects. *Int. Journal of Hydrogen Energy*, 27:1217–1228.
- Melis, A. and Happe, T. (2001). Hydrogen production. Green algae as a source of energy. *Plant Physiology*, 127(3):740–748.
- Moore, J., Stanitski, C., and Jurs, P. (2009). *Principles of Chemistry: The Molecular Science*. Available Titles OWL Series. Cengage Learning.
- Reger, D., Goode, S., and Ball, D. (2009). *Chemistry: Principles and Practice*. Available Titles OWL Series. Brooks/Cole.
- Sawada, S., Kuninaka, M., Watanabe, K., Sato, A., Kawamura, H., Komine, K., Sakamoto, T., and Kasai, M. (2001). The mechanism to suppress photosynthesis through end-product inhibition in single-rooted soybean leaves during acclimation to CO<sub>2</sub> enrichment. *plant and cell physiology*, 42(10):1093–1102.
- Stitt, M. (1991). Rising CO<sub>2</sub> levels and their potential significance for carbon flow in photosynthetic cells. *Plant, Cell & Environment*, 14(8):741–762.
- Trambouze, P. and Euzen, J. P. (2004). *Chemical Reactors*. Institut Français du Pétrole Publications. Editions Technip.
- Tsygankov, A. A., Kosourov, S., Seibert, M., and Ghirardi, M. L. (2002). Hydrogen photoproduction under continuous illumination by sulfur-deprived, synchronous *Chlamydomonas reinhardtii* cultures. *Int. Journal of Hydrogen Energy*, 27:1239–1244.